Article:
Al Naim, A., Hobson, A., Grant, R.T. et al. (2013) Water-gated organic nanowire transistors. Organic Electronics, 14 (4). pp. 1057-1063. ISSN: 1566-1199

https://doi.org/10.1016/j.orgel.2013.01.024

Water- gated organic nanowire transistors

Abdullah Al Naim[1)*], Richard T. Grant[1)], Antonis Dragoneas[1)], Adam Hobson[1)], Mark Hampton[2)], Chris Dunscombe[2)], Tim Richardson[1)], J. Emyr Macdonald[2)], and Martin Grell[1)]

[1)]Department of Physics and Astronomy, University of Sheffield, Hicks Building, Hounsfield Road, Sheffield, South Yorkshire, United Kingdom, S3 7RH

[2)]School of Physics and Astronomy, Cardiff University, The Parade, Cardiff CF24 3AA, United Kingdom

* corresponding author

Keywords: Thin film transistor, electrolyte, nanowire, organic semiconductor.

Abstract:
We gated both p- type, and n- type, organic nanowire (NW) films with an aqueous electric double layer (EDL) in thin- film transistor (TFT) architectures. For p- type NWs, we used poly(3-hexylthiophene) (P3HT) NWs grown via two different routes. Both can be gated with water, resulting in TFTs with threshold lower than for conventionally cast P3HT films under the same gating conditions. However, TFT drain currents are lower for NWs than for conventional P3HT films, which agrees with similar observations for 'dry' gated TFTs. For n- type NWs, we have grown 'nanobelts' of poly(benzimidazobenzophenanthroline) (BBL) by a solvent / non- solvent mixing route with later displacement of the solvent, and dispersion in a non- solvent. Water- gating such films initially failed to give an observable drain current. However, BBL nanobelts can be gated with the aprotic solvent acetonitrile, giving high n- type drain currents, which are further increased by adding salt. Remarkably, after first gating BBL NW films with acetonitrile, they can then be gated by water, giving very high drain currents. This behaviour is transient on a timescale of minutes. We believe this observation is caused by a thin protective acetonitrile film remaining on the nanobelt surface.

Introduction

A thin- film transistor (TFT) architecture has been widely used in particular with non-conventional semiconductors, e.g. amorphous Si [1], organic semiconductors (OSCs) [2], and precursor- route inorganic semiconductors [3,4]. Therein, a thin film of an intrinsic (i.e., undoped) semiconductor is gated by a voltage applied to a gate electrode that is not directly in contact with the semiconductor, but separated from it via a gate medium. When the gate voltage exceeds a threshold, the 'field effect' generates a charge carrier accumulation layer at the semiconductor / gate medium interface, with a resulting increase in conductivity up to several orders of magnitude. The properties of the gate medium, in particular its specific capacitance and density of carrier traps at the insulator/semiconductor interface, are crucially important to the TFT's performance [2,5]. Traditionally, the gate medium was a solid dielectric. Recently, however, electrolytes have also been used as gate media. Under applied gate voltage, mobile ions form an electric double layer (EDL) at the gate medium / semiconductor interface, which displays very high specific capacitance, generating a strong electric field near the interface, even at gate voltages below 1V. Solid electrolytes and ionic liquids have been used as gate media for hole [6,7]- as well as electron- transporting [8] OSCs. An interesting development is the discovery of Kergoat *et al.* that even deionised (DI) water can act as a gate medium for OSCs [9]. This discovery has inspired attempts to develop OSC- based TFT sensors for the detection of waterborne analytes, wherein the water sample under investigation is used as the TFT's gate medium [10]. The specific capacitance of the EDL in deionised water has been estimated as 3 $\mu F/cm^2$ [9]; however, the capacitance of EDLs is a notoriously complicated function of frequency, geometry and ion concentration [11], and this figure is best taken only as an order- of-magnitude estimate.

Another recent line of OSC TFT research is the introduction of organic nanowires (NWs). NWs are long, needle-shaped crystals that may grow when some OSCs (namely those with a slip-stacked crystal motif) undergo suitable physicochemical treatment while in solution, e.g. thermal cycles, or addition of non- solvent. Depending on the material, and growth conditions, some variations on the NW morphology have also been observed, e.g. flat 'nanobelts' [12] or curved 'nanofibres' [13]. We will here refer to all of these related morphologies as 'nanowires' as generic term, except when discussing a specific sample. After formation, NWs may form stable suspensions in their growth medium and can be processed into films by spin- or drop- casting, similar to film deposition from OSC solutions. However, the morphologies of resulting films are distinctly different from the smooth, uniform films obtained when casting OSCs from proper solutions. Depending on casting conditions and NW density in the growth medium, films may contain isolated single wires, lightly overlapping wires or a dense

multilayer NW 'mesh'. The literature on organic NWs (and related morphologies) includes many reports on TFTs; these have been comprehensively reviewed by Briseno *et al.* [14].

The NW morphology implies a large OSC surface area, and consequently, has led to remarkable sensitivity enhancement of chemiresistor devices that employ NWs, compared to devices using the same OSC in the form of uniform, solution-cast films [13,15]. It is therefore tempting to implement organic NWs as the active layer in electrolyte- gated OSC TFTs. To date, however, no electrolyte- gated NW OSC field-effect TFTs have been reported. The work of Wanekaya *et al.* [16], despite its title, does report on an organic electrochemical transistor (OECT), rather than a field effect transistor, and requires a strongly acidic medium. For the classification, and relative merits, of OECTs *vs.* organic TFTs, see for example the reviews of Inganäs [17], and Owens and Malliaras [18].

Here, we demonstrate water- gated organic NW field-effect TFTs using NWs grown from both p- type, and n- type, OSCs. As p- type organic semiconductor, we have chosen regioregular poly(3-hexylthiophene) (P3HT), an OSC widely used for organic TFTs [2]. P3HT is also known for its ability to grow NWs [19], and water-gated field effect TFTs using P3HT films cast from chloroform have been demonstrated by Kergoat *et al.* [9]. As n- type organic semiconductor, we have selected poly(benzimidazobenzophenanthroline) (BBL). BBL can act as n- type material in organic TFTs with good mobility (μ_e = 0.1 cm^2/Vs) [20], and Briseno *et al.* [12] have reported on the growth of BBL 'nanobelts'. BBL possesses a rather deep 'lowest unoccupied molecular orbital' (LUMO) of - 4.0 eV [21], which allows reasonable electron injection even from high work function metals, and may make BBL consistent with water- gating, despite the potential trapping of electrons by water and/or oxygen: Nicolai *et al.* [22] recently suggested from theoretical calculations that such trapping can be avoided when the LUMO is more than 3.6 eV below vacuum level.

Experimental

Nanowire growth: "CB-P3HT" NWs were grown from regioregular P3HT (rrP3HT) (sourced from Ossila) in 5 mg/mL chlorobenzene (CB) solution. CB was initially heated to 80 °C and agitated to allow solution; solutions were then filtered through a 0.45 µm PTFE syringe mounted filter, and left to mature in the dark at ambient temperature for several weeks or months. "Anisole-P3HT" NWs were prepared via a variation on the whisker method [19]. 5mg of rrP3HT (sourced from ADS dyes) were dissolved in 1ml of Anisole. The solution was heated to 90 °C until fully dissolved and allowed to cool to room temperature over a duration of approximately 1 hr, and then left to mature for

three days. Thermal cycles and maturing were carried out in sealed bottles to avoid solvent evaporation. “BBL” nanobelts were grown from poly(benzimidazobenzophenanthroline) (BBL) (sourced from Sigma Aldrich) dissolved at 0.2 mg/ml in methane sulfonic acid (MSA). BBL nanobelt growth was driven by the drop- wise addition of a non- solvent mixture (chloroform/methanol 4:1) to the solution of BBL in MSA whilst stirring continuously, as described in [12]. Due to the strong (acid/base) interactions between MSA and BBL, it is likely that some residual MSA remains incorporated in the resulting BBL NWs; however, this will also be the case for BBL films cast from MSA (*cf.* the casting procedure reported by Babel and Jenekhe [21], which also relies in the displacement of MSA with a non- solvent).

Both chloroform and methanol are highly volatile, while MSA is not; hence MSA needs to be removed from the resulting BBL NW suspension prior to casting films, otherwise MSA would re- dissolve NWs during casting. Therefore, BBL NW suspensions were centrifuged for 10 minutes at ≈ 910g to make NWs settle to the bottom of a phial. Clear excess solvent was carefully pipetted off from above the settled NWs, before being replenished with either methanol, ethanol, or isopropanol. BBL NWs dispersed well in alcohols, and we later did not find any systematic differences in the electrical behaviour of BBL nanobelt films cast from either dispersion agent. BBL NWs did not disperse in water though, so we could not prepare aqueous BBL NW formulations. This process was then repeated three times. Eventually, this resulted in BBL NWs suspended in clear carrier solvent almost free of MSA, and with no residual dissolved BBL that has not been incorporated into NWs.

NW TFT preparation: We prepared OSC NWs onto Au electrode pairs of width W = 2 mm, separated by a channel of length L = 10 µm (for P3HT samples), and of length 20 µm for BBL samples, to account for the larger size of BBL nanobelts, giving ratios W/L = 200 for P3HT; W/L = 100 for BBL. 100 nm thick gold contacts were prepared by photolithography onto insulating SiO_2 substrates after depositing 10 nm of Cr as adhesion layer. The contact geometry, sketched in Fig. 1, uses 0.1mm thin wires to connect S/D contacts to distant contact pads. This design limits overlap area between Au contacts and the water droplet applied later to ~ 0.4 mm^2, thus minimising parasitic currents across the droplet, while still allowing convenient contacting. CB-P3HT NWs were spun at 5000 rpm onto contact substrates without prior substrate treatment. Anisole-P3HT NWs were spun at 2000 rpm, and BBL nanobelts were drop- cast by repeatedly applying ≈ 2 µL droplets of nanobelt dispersion onto substrates and allowing solvent evaporation, until contacts were completely covered with nanobelts.

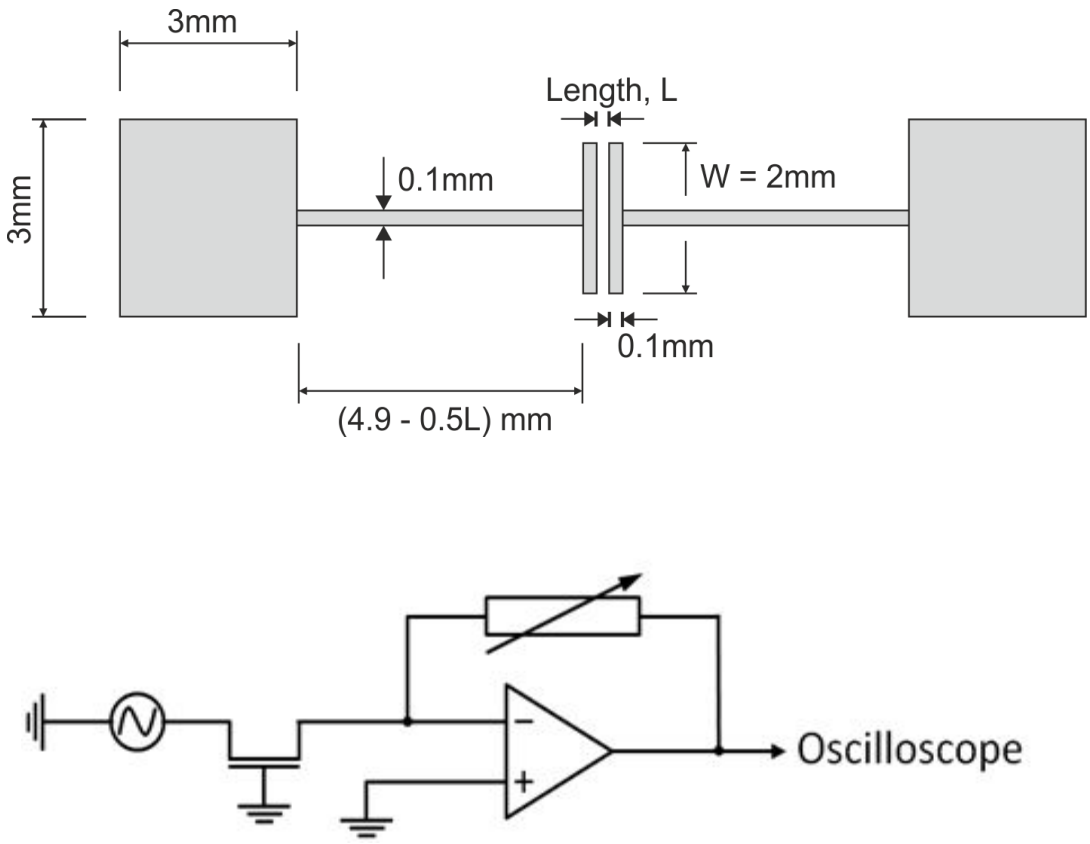

Fig. 1a: Contact geometry used for water- and solvent- gated transistors. Channels of length L = 10 or 20 μm and width W = 2 mm, are linked to distant contact pads by thin (100 μm) connecting wires. **b:** Electric scheme for TFT characterisation. The TFT is driven by a sinusoidal source voltage, V_S, with gate grounded, and drain on the virtual ground input of a current- to- voltage (I/V) converter, realised by an operational amplifier with variable feedback resistor (resistance decade box). A detailed description is in [24].

Nanowire film characterisation: For nanowire AFM characterisation, a Veeco Dimension 3100 was used to obtain height and phase images of spin- cast P3HT NW films. The controller used on all AFM images was a Nanoscope IIIa controller with a Basic Extender. For all images, we used a standard tapping mode cantilever (Bruker TESPA, k = 42 N/m, resonant frequency 320 kHz). The full specifications for these cantilevers can be found at [29].

Electrolyte- gating and electrical characterisation: For electrical testing, two Tungsten (W) needles were dropped onto the substrate's contact pads using Karl Süss probeheads, so these could act as the TFT 'source' (S) and 'drain' (D) electrodes. As gate media, we used deionised water, and acetonitrile (HPLC quality from Aldrich). For

gating,the fixed volume (≈ 2 µL) of droplet of DI water or acetonitrile was applied over the channel region from a microlitre syringe. A third W needle was bent into a 'L'-shape and was dropped onto the droplet with the foot of the L overlapping the channel, to act as 'gate' (G) contact, as in [23]. Transistors were driven electrically by applying a sine drive voltage ($V_S(t)$) to S, connecting G to ground, and D to the virtual ground of a current/voltage (I/V) converter with a resistance decade box as variable feedback resistor, R_f. The electric scheme is shown in Fig. 1b. The peak voltage of V_S was 0.8 V for water and 1.1 V for acetonitrile. A low frequency of 1Hz or less was chosen to account for the slow build- up of the EDL [9]. $V_S(t)$ and the output voltage ($V_{OUT}(t)$) of the I/V converter were recorded on a storage oscilloscope, V_{OUT} being proportional to the saturated drain current ($I_{SD}(t)$) that the TFT under test drives to virtual ground, $V_{OUT} = -R_f I_{SD}$. The chosen setup is 'blind' to gate leakage currents. Together, $V_S(t)$ and $I_{SD}(t)$ constitute the TFT's saturated transfer characteristic, albeit parametric in time rather than explicit. A detailed description of the measurement scheme, and the evaluation of TFTs directly from parametric saturated transfer characteristics, is given in [24]. Alternatively, time can easily be eliminated to retrieve saturated transfer characteristics in 'traditional' form, as in Fig. 3b below. For the characterisation of subthreshold behaviour, and output characteristics, a conventional TFT characterisation setup with two Keithley source/measure units was used.

Results and Discussion

Fig. 2 shows the morphologies of the different NW films employed here. Fig. 2a shows a film cast from P3HT NWs grown in chlorobenzene ('CB-P3HT NWs'). NWs are rather rigid, typically a few µm long, and they do lightly overlap. Fig. 2b shows 'Anisole-P3HT' NWs, which display a rather different morphology: Several NWs radiate out from a central 'seed', NWs are longer than CB-P3HT NWs, and curved. Different NW growth protocols thus lead to different morphologies. Fig. 2c shows the morphology of BBL 'nanobelts' grown, purified, and processed along the somewhat more intricate procedure described in the experimental section. BBL grows into flat ribbons ('belts'), rather than one- dimensional wires like P3HT, and ribbons are larger than NWs; these are hence adequately imaged by optical microscopy, rather than AFM (note the different scale in Fig. 2c). We did not observe any systematic morphological differences between the different solvents (methanol, ethanol, isopropanol) used to displace MSA.

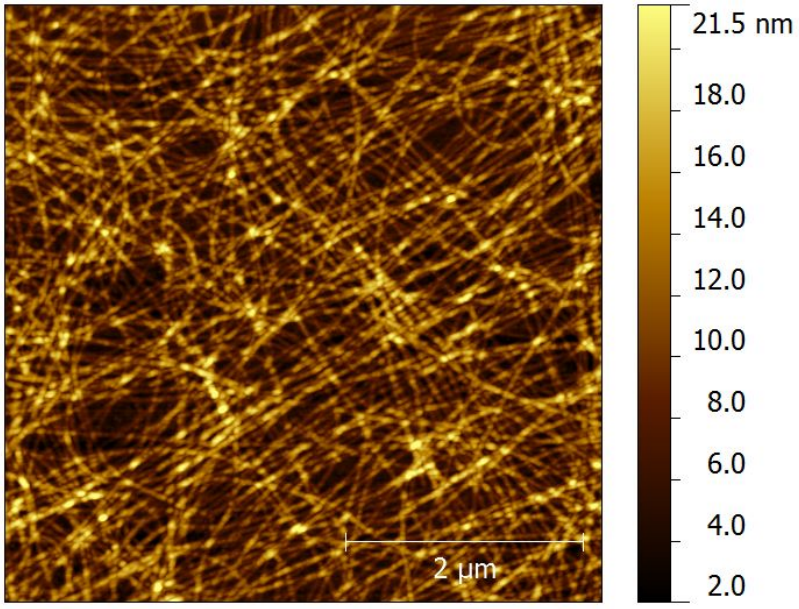
21.5 nm
18.0
16.0
14.0
12.0
10.0
8.0
6.0
4.0
2.0
2 µm

(a)

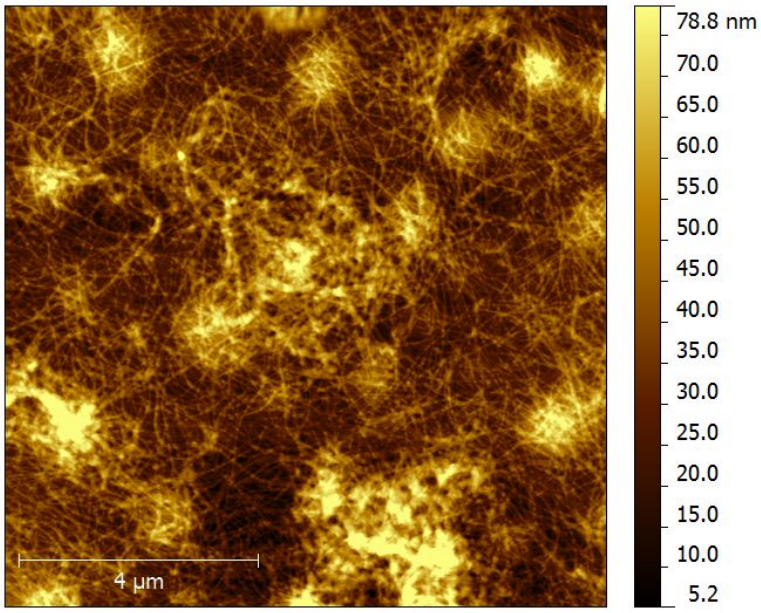
78.8 nm
70.0
65.0
60.0
55.0
50.0
45.0
40.0
35.0
30.0
25.0
20.0
15.0
10.0
5.2
4 µm

(b)

(c) 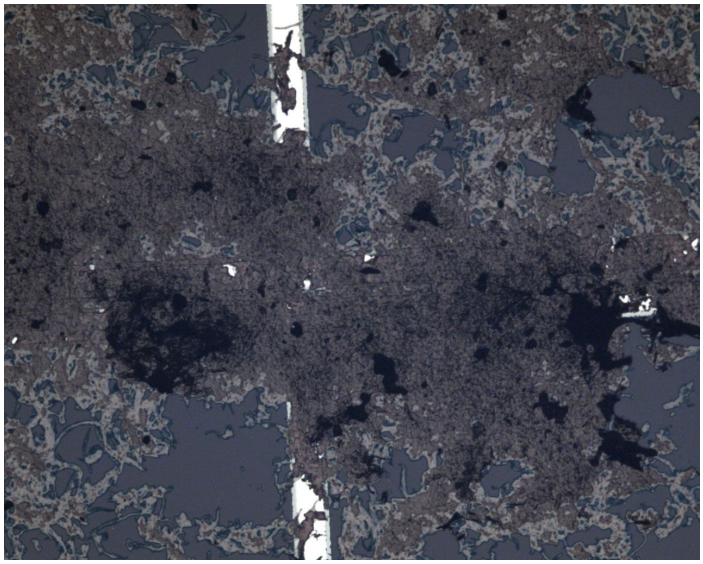

Fig. 2a: AFM image of CB-P3HT NWs. 5 mg/ml rrP3HT in chlorobenzene solution was matured for 5 months to allow NW growth, then spun at 5000 rpm onto the TFT substrate. Image shows an area in the channel (channel length 10μm). **2b:** AFM image of Anisole-P3HT NWs spun onto TFT substrate. **2c:** Optical micrograph of BBL nanobelts cast from isopropanol, covering the channel completely. Parts of the connecting wires (*cf.* Fig. 1) are visible; these are 100 μm wide.

In Fig. 3a, we show the saturated transfer characteristics parametric in time for CB-P3HT, and Anisole-P3HT, when gated with DI water, and driven from the source. For comparison, we also include the characteristics of a conventional P3HT film under otherwise the same conditions. The current observed for the conventional P3HT film agrees within 25% with the value reported previously by Kergoat *et al.* [9] after the different channel geometry is taken into account. Fig. 3a shows that both CB-P3HT and Anisole-P3HT NW films display low threshold voltage TFT characteristics, with a clearly distinct 'on'- cycle for positive V_S / 'off' cycle for negative V_S, as it is typical for p- type organic transistors driven from the source contact [24]. The absence of a phase lag between drive voltage (V_S) and drain current (I_{SD}) peaks confirms that 1 Hz drive frequency is sufficiently slow for quasi- static TFT characteristics. The low current in the 'off' cycle shows that very little parasitic current flows across the gate droplet (rather than the semiconductor), due to the small overlap- area between contacts and water droplet. The saturated drain current is somewhat higher for CB-P3HT NWs than for Anisole-P3HT, probably due to the morphological differences (straight CB-P3HT NWs *vs*. curved, star- shaped Anisole-P3HT NWs). However, both are significantly lower compared to conventional P3HT films under water gating (note the scaling used in Fig. 3a; current (I_{SD}) for both NW films is magnified ten- fold). We note that the current

observed for the conventional P3HT film agrees within 25% with the value reported previously by Kergoat *et al.* [9] after the different channel geometry is taken into account.

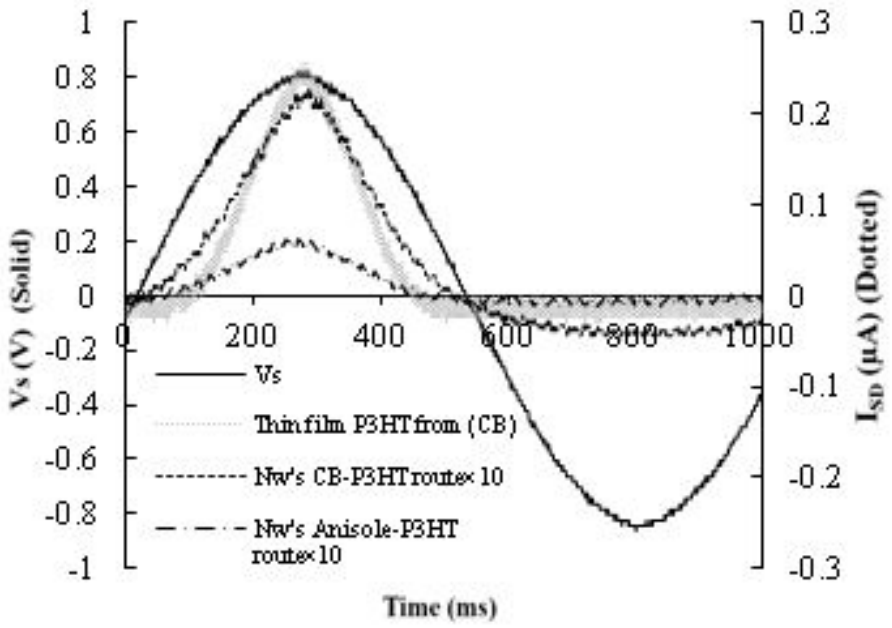

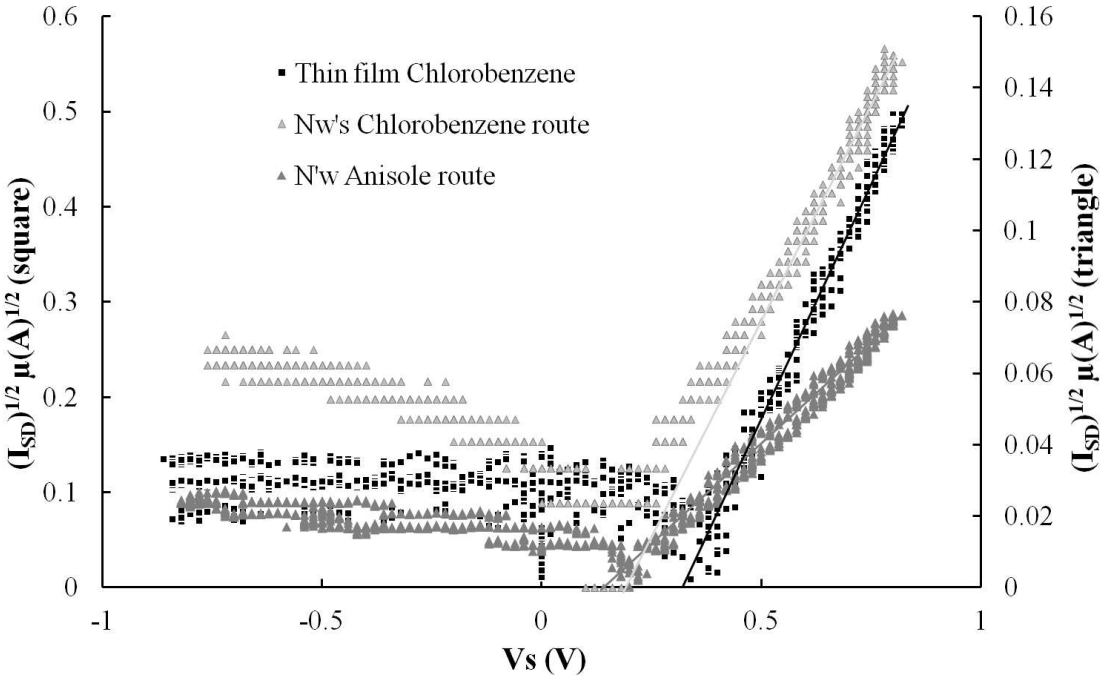

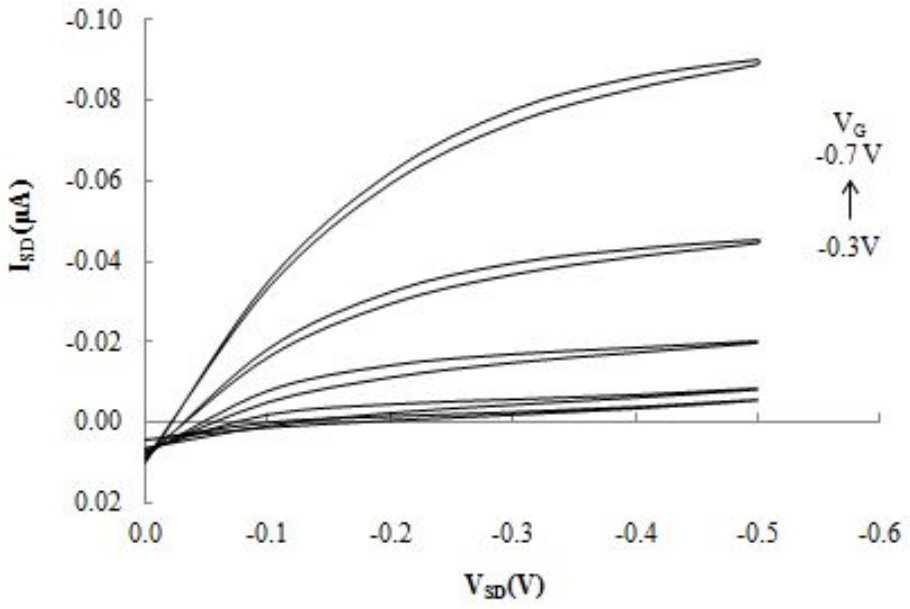

Fig. 3: a.) Sinusoidal drive voltage, $V_S(t)$, and resulting TFT source- drain current $I_{SD}(t)$, for water- gated CB-P3HT NW, and Anisole-P3HT NW, films (as shown in Fig.s 2a,b). Drain current $I_{SD}(t)$ calculated from V_{OUT} of the I/V converter by $V_{OUT} = -R_f I_{SD}$. I_{SD} for a conventional P3HT film is also shown. I_{SD} for both NW TFTs is magnified tenfold. **b.)** Saturated transfer characteristics for CB-NW, and Anisole-NW films, in the form $I_{SD}^{1/2}$ *vs.* V_S; derived from 3a by eliminating time. The threshold voltage, V_T, is read from the intercept of a straight line fitted for high V_S during the 'on' cycle with a flat line extrapolated from V_S in the 'off' cycle. **c.)** Output characteristics for water- gated CB-NW TFT, recorded with a conventional TFT characterisation setup. The linear $I_{SD}(V_{SD})$ behaviour for $V_{SD} << V_G$ shows that contact resistance is negligible in this case.

The low currents observed for water- gated organic NW TFTs agree with similar observations on 'dry' organic NW TFTs, which despite of the high carrier mobility along the axis of individual NWs typically display rather low source- drain currents, *cf.* the examples shown in the review by Briseno *et al.* [14].

This is due to the often incomplete filling of the channel width (W) with NWs (e.g. Fig. 2a), and the need for carriers to overcome NW-NW junctions within the channel. It is not quite clear if it is the different morphology, or a lower channel 'fill- factor', that leads to the even lower current in Anisole-NWs. However, while contact problems between bottom contacts and NWs are often evident in the NW TFT output characteristics of 'dry'- gated NW TFTs by an upward curvature rather than linear $I_{SD}(V_{SD})$ behaviour for

V_{SD} << V_G [12, 14], contact resistance is negligible here, as can be seen from the output characteristics in Fig. 3c. Also, limited penetration of the gate water into the hydrophobic P3HT NW mesh, leading to only superficial gating, is unlikely to be the cause of low drain currents: When we added some detergent to a gate droplet, surface tension visibly relaxed, which should lead to improved wetting. However, drain current decreased even further.

Despite the low drain currents, Fig. 3a shows that organic NW films can be gated within the electrochemical window of water to realise electrolyte- gated organic NW TFTs. In fact, the threshold voltage (V_T) is lower for NW TFTs than for conventional P3HT films, as can be seen more clearly from the $(I_{SD})^{1/2}$ *vs*. V_S plots shown in Fig. 3b. This gives V_T = (0.38 ± 0.02) V for the conventional P3HT films, V_T = (0.27 ± 0.02) V for Anisole-P3HT, and (0.22 ± 0.02) V for CB-P3HT. Note that attempts to calculate a carrier mobility for NW TFTs are ill- advised due to the unknown channel fill- factor, and the ambiguity in quantifying EDL capacitance.

The NW morphology is therefore accessible in principle for water- gated p- type organic TFT sensor devices, to exploit the large surface area of NWs for sensitivity enhancement [13,15].

We have also attempted water- gating of n- type NWs. BBL 'nanobelts' were grown and deposited as described in the experimental section, see Fig. 2c for their morphology. The option to use n- type, as well as p- type, TFTs, is generally desirable for organic electronics, to mimic 'CMOS' type devices like complementary inverters [25]. In the context of sensor technology, dry n- type OSC TFTs have been shown to be more sensitive to some odours than p- type TFTs [26], and n- type electrolyte- gated TFTs are turned on by a cationic (rather than anionic) EDL, hence n- type OSCs have an advantage over p- types for the sensing of waterborne cations. Initially, however, we had no success with water- gating BBL nanobelts, presumably due to electron trapping by -OH groups, despite the low LUMO. Therefore, we have used acetonitrile, as an alternative to water, as gate medium for BBL nanobelts. Acetonitrile (H_3C-C≡N) is aprotic (free of -OH groups), yet highly polar. It is widely used in electrochemistry for its aprotic character, wide electrochemical window, and ability to dissolve salts [27]. We have already shown acetonitrile- gated PBTTT (p- type) and ZnO (n- type) TFTs [28]. Fig. 4a shows the saturated transfer characteristics of acetonitrile (HPLC grade)- gated BBL nanobelt TFTs. Note the maximum drive voltage can be selected somewhat higher than for water gating due to the bigger electrochemical window of acetonitrile.

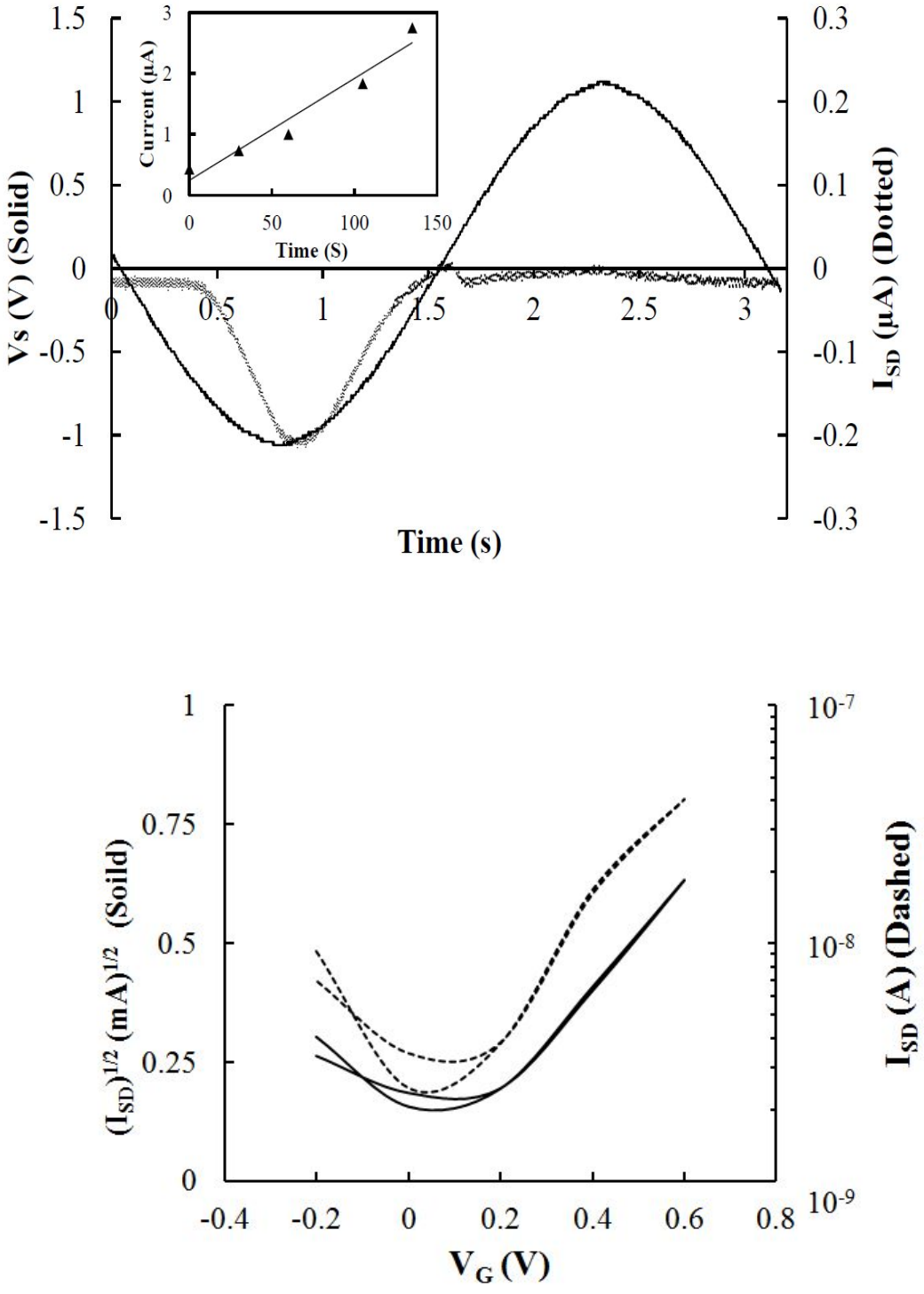

Fig. 4: a.) Sinusoidal drive voltage, $V_S(t)$, and the resulting TFT source- drain current $I_{SD}(t)$, for acetonitrile- gated BBL NWs, calculated from V_{OUT} of the I/V converter by $V_{OUT} = -R_f I_{SD}$. **Inset:** TFT 'on' current at maximum drive voltage, $I_{SD}(V_S = 1.1\ V)$, for

acetonitrile-gated BBL TFT as a function of time, while a minute flake of NaCl dissolves in the gate droplet. **b.)** Saturated transfer characteristics in the form $I_{SD}^{1/2}$, and log I_{SD}, *vs* V_G, measured by a conventional setup. Solid line: $I_{SD}^{1/2}$ scale; dashed line: log I_{SD} scale.

We find clearly distinct 'on'- cycle for negative V_S / 'off' cycle for positive V_S, as is typical for n- type organic transistors driven from the source contact [26]. These characteristics remained stable for 5 to 6 minutes. Threshold voltages can be evaluated similarly as for P3HT in Fig. 3b, giving V_T = (0.22 ± 0.02) V. The highest accessible saturated drain currents (limited by the electrochemical window of acetonitrile) are in the range 200...400 nA for different samples, larger than for water- gated P3HT NWs, but similar to the maximum drain current observed for dry- gated BBL nanobelt TFTs (limited by the dielectric breakdown of the dry gate insulator) with similar nanobelt morphology, and device geometry (~ 360 nA, [12]). However, here we achieve this current with a gate voltage of only 1.1 V , while Briseno *et al.* [12] required 80 V to reach maximum current. This confirms that electrolyte- gated n- type OSC NW TFTs are viable, as long as a suitable (i.e., aprotic) gate medium is used. Due to the high EDL capacitance, maximum current is reached at much lower voltage than for a 'dry' gate insulator. Also, unlike for P3HT, saturated drain currents in BBL nanobelt TFTs are similar to those found for solution- cast BBL film transistors of similar geometry (~ 300 nA [21]). This indicates near- complete filling of the channel with nanobelts, which is not the case for P3HT nanowires, *cf.* Fig. 2.

We have recently concluded [28] that the ability of some organic solvents to act as EDL gate media results from minute traces of dissolved salts. In fact, when the HPLC acetonitrile gate droplet is allowed to evaporate, I_{SD} at first somewhat increases, probably because trace salts become more concentrated (off course, as the gate droplet dries up completely, the transistor eventually fails). We have therefore attempted to enhance maximum current in acetonitrile- gated BBL nanobelt TFTs by deliberately adding salt to acetonitrile. The inset to Fig. 4a shows the 'on' current I_{SD}(1.1 V) of the same BBL nanobelt TFT over time, while a minute flake of NaCl dissolves in the gate medium. As the salt slowly dissolves, I_{SD} increases more than 5- fold, eventually reaching almost 3 µA.

When we again attempted to gate a BBL nanobelt film with water, after it had first been gated with acetonitrile that was then allowed to dry up, we surprisingly found that water gating was now effective, leading to TFTs with unusually high saturated drain current. Fig. 5a shows the near- ideal output characteristics of such devices, displaying a saturated drain current of more than 70 µA at less than 1V, which increases further over

a few minutes (Fig. 5b) to almost 200 μA, an almost 3 order- of- magnitude increase over the saturated drain current observed for the same film under prior acetonitrile-gating. When data from Fig. 5a are evaluated with the standard saturated drain current equation for a TFT (assuming completely filled channel), and assuming a gate capacitance of C_i = 3 μF/cm^2 [9], we find electron mobility μ_e= 1.4 cm^2/Vs, higher than reported previously for solution- cast BBL films (μ_e = 0.1 cm^2/Vs) [21], or dry- gated BBL nanobelt TFTs ($\mu_e < 10^{-2}$ cm^2/Vs) [11].

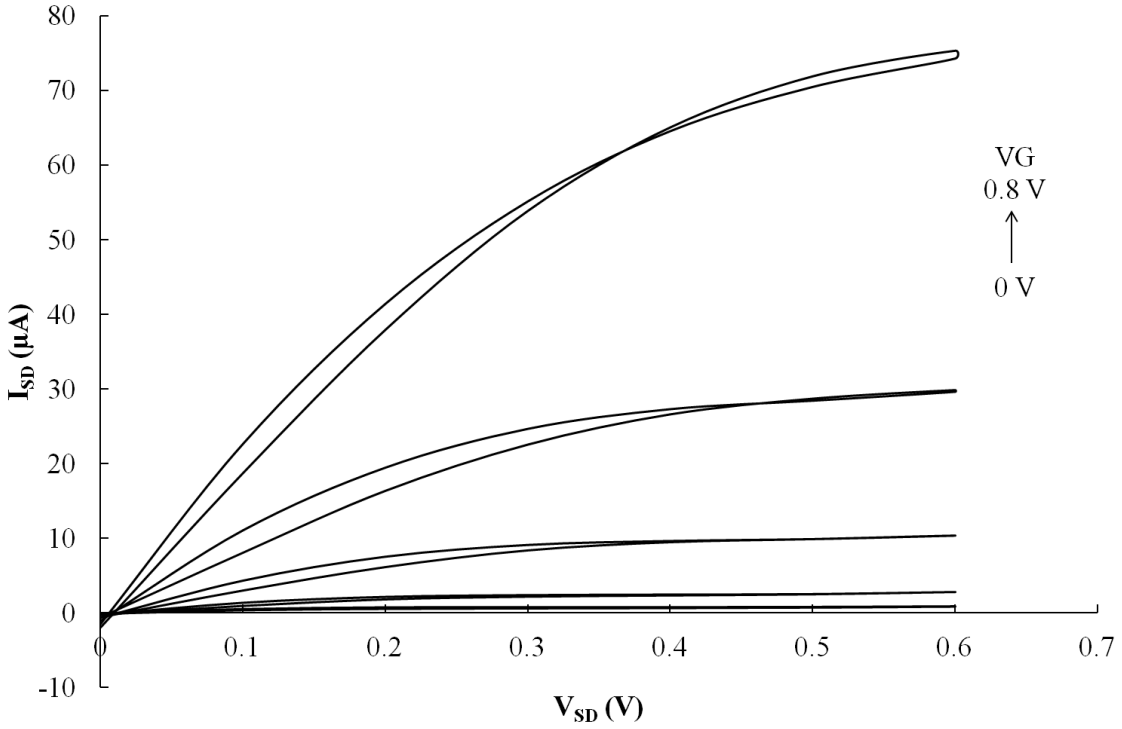

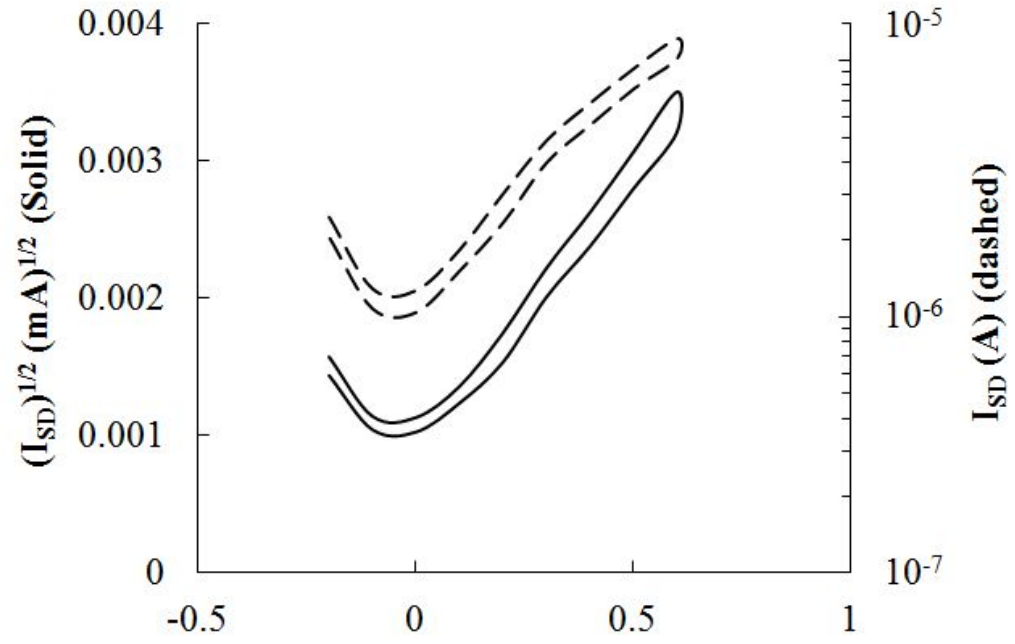
0.004
0.003
0.002
0.001
0
-0.5
0
0.5
1
10^{-5}
10^{-6}
10^{-7}
$(I_{SD})^{1/2}$ (mA)$^{1/2}$ (Solid)
I_{SD} (A) (dashed)

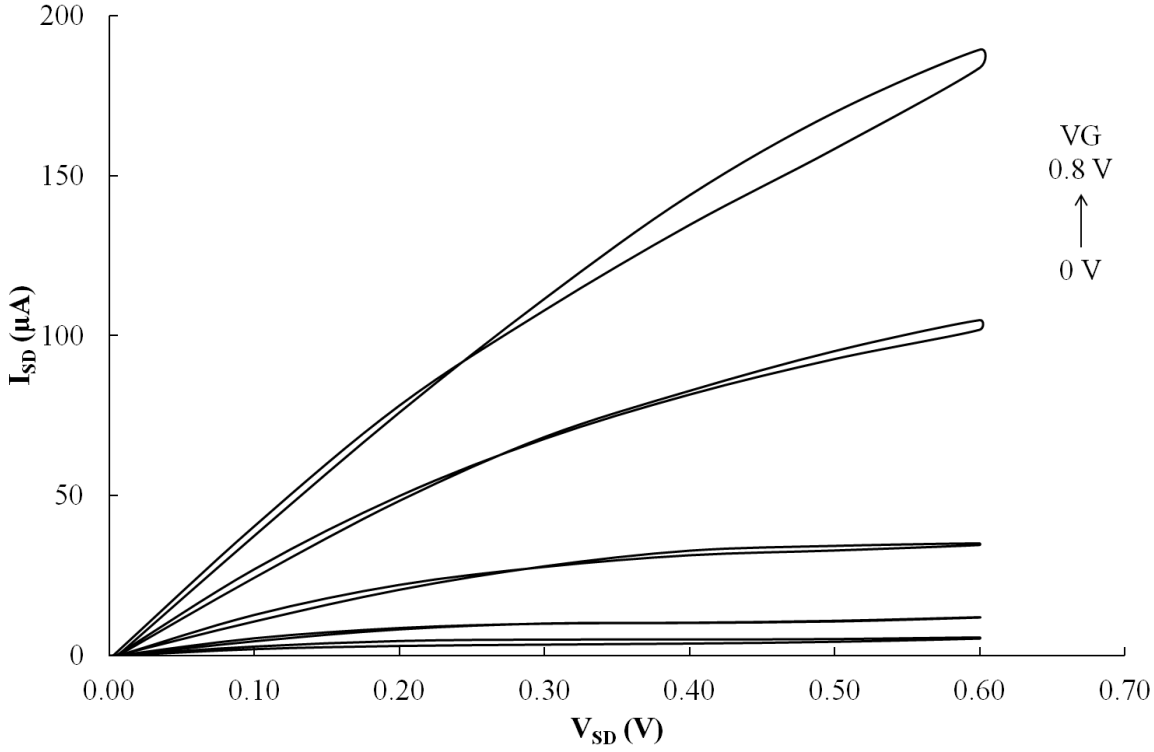
200
150
100
50
0
0.00
0.10
0.20
0.30
0.40
0.50
0.60
0.70
I_{SD} (μA)
V_{SD} (V)
VG
0.8 V
0 V

Fig. 5: Output **(a)**- and transfer (V_{SD}=0.8V) **(b)** characteristics of BBL nanobelt film gated with water after acetonitrile dried up, immediately after applying the water gate droplet. **c:** 2 min. after applying the droplet. Note the droplet has not evaporated. Output characteristics are shown for increasing and decreasing V_{SD}.

At longer times, the TFT properties deteriorate. Current remains high, but output characteristics become largely independent of gate voltage. The device behaves similar to a resistor, rather than a transistor. When the gate droplet is left to dry up completely, and then is replaced with fresh water, the characteristics shown in Fig. 5a cannot be recovered. However, we repeated the entire experimental sequence on an independently prepared second sample, with very similar results.

We suggest that the acetonitrile 'conditions' the BBL nanobelts, leaving a very thin acetonitrile layer on the surface that later shields them from direct contact with water, and its -OH groups that are detrimental to electron transport. Over a period of minutes, the protective layer dissolves into the water droplet. We agree this is not a full explanation for our remarkable observations.

Summary and conclusions

We conclude that both p- type, and n- type, organic NW films can be gated with the EDL that forms at the interface between NWs, and gate medium. As p- type NWs, we have grown NWs from P3HT solutions via two different routes, using different solvents (CB and Anisole) as growth media, and thermal cycling, or simply long- term maturing. Different growth media resulted in NWs with different morphologies. Films of both morphologies can be gated with water without prior conditioning, resulting in TFTs with very low threshold voltages; even lower than for conventionally cast P3HT films. The resulting saturated drain currents are lower than for conventional P3HT films; however, this is similar to the observations in 'dry' NW transistors [14]. Reduced drain currents are probably due to the partial filling of the transistor channel, and injection problems at the metal / NW contacts. We propose water- gated NW TFTs for use in sensors for waterborne analytes, as the high surface area of NWs promises higher sensitivity than conventional organic semiconductor films. As n- type NWs, we have grown 'nanobelts' from the n- type organic semiconductor, poly(benzimidazobenzophenanthroline) (BBL) by a solvent / non- solvent mixing route with later displacement of the solvent in favour of a non- solvent as dispersion medium. When gating of such films with water was attempted, we initially did not observe a resulting drain current. However, BBL nanobelts can be gated with an aprotic gate medium (acetonitrile), to give n- type EDL

gated organic field effect nanobelt TFTs. Drain current was similar to that observed in dry- gated BBL nanobelt TFTs, and dry- gated TFTs using conventionally cast BBL films. However, this was achieved at substantially lower gate voltage, and could be further enhanced by adding salt to the gate medium. Remarkably, BBL NW films can also be gated by water (a protic gate medium) after first conditioning them with acetonitrile. Such TFTs display very high drain currents; however this remarkable behaviour is transient on a timescale of minutes. While we have no detailed explanation of this behaviour, we believe it may be related to a thin protective acetonitrile film on the nanobelt surface that remains from the prior conditioning. We propose to explore more permanent protective films.

Acknowledgements: Abdullah F Al Naim thanks the Saudi Cultural Bureau in London, UK, and King Faisal University in Al Hassa, Saudi Arabia, for the provision of a PhD scholarship. A Dragoneas thanks the EC for the provision of an 'Early Stage Researcher' fellowship under the 'FlexSmell' initial training network (ITN). Adam Hobson and Mark Hampton would like to thank the UK Engineering and Physical Sciences Research Council (EPSRC) for funding their PhD scholarships. The research was partly funded by EPSRC grant EP/I006052/1. The authors would also like to thank Dr Nic Mullin and Prof Jamie Hobbs for the use of their AFM laboratory, and assistance and advice from Dr Nic Mullin.

References:

[1] Jerzy Kanicki, Amorphous & Microcystalline Semiconductor Devices Volume II: Materials and Device Physics. (Artech House, Inc., 1992).
[2] (a) G Horowitz, *Adv. Mater.* **10**, 365 (1998); (b) C D Dimitrakopoulos, P R L Malenfant, *Adv. Mater.* **14**, 99 (2002); (c) H Sirringhaus, *Proc. IEEE* **97**, 1570 (2009)
[3] B S Ong, C Li, Y Li, Y Wu, R Loutfy, *JACS* **129**, 2750 (2007)
[4] S - J Seo, C G Choi, Y H Hwang, B S Bae, *J. Phys. D: Appl. Phys* **42**, 035106 (2009)
[5] J Veres, S D Ogier, S W Leeming, D C Cupertino, S M Khaffaf, *Adv. Func. Mater.* **13**, 199 (2003)
[6] E Said, X Crispin, L Herlogsson, S Elhag, N D Robinson, M Berggren, *APL* **89**, 143507 (2006)
[7] S Ono, S Seki, R Hirahara, Y Tominari, J Takeya, *APL* **92**, 103313 (2008)
[8] T Uemara, M Yamagishi, S Ono, J Takeya, *APL* **95**, 103301 (2009)
[9] L Kergoat, L Herlogsson, D Braga, B Piro, M C Pham, X Crispin, M Berggren, G Horowitz, *Adv. Mater.* **22**, 2565 (2010)
[10] L Kergoat, B Piro, M Berggren, M C Pham, A Yassar, G Horowitz, *Organic Electronics* **13**, 1 (2012)
[11] E Gileadi, E Kirowa-Eisner, J Penciner, 'Interfacial Chemistry: An Experimental

Approach', Addison-Wesley, USA 1975
[12] A L Briseno, S C B Mannsfeld, P J Shamberger, F S Ohuchi, Z Bao, S A Jenekhe, Y Xia, *Chem. Mater.* **20***, 4712* (2008)
[13] J Huang, S Virji, B H Weiller, R B Kaner, *JACS* **125**, 314 (2003)
[14] A L Briseno, S C B Mannsfeld, S A Jenekhe, Z Bao, Y Xia, *Materials Today* **11**, 38 (2008)
[15] A Dragoneas, M Hampton, J E Macdonald, M Grell, *Sensor Letters,* accepted
[16] A K Wanekaya, M A Bangar, M Yun, W Chen, N Y Myung, A Mulchandani, *J. Phys. Chem. C* **11**, 5218 (2007)
[17] O Inganäs, *Chem. Soc. Rev.* **39**, 2633 (2010)
[18] R M Owens, G G Malliaras, *MRS Bulletin* **35**, 449 (2010)
[19] K J Ihn, J Moulton, P Smith. *J. Polym. Sci. Pol. Phys.*, **31**, 735 (1993)
[20] A L Briseno, F S Kim, A Babel, Y Xia, S A Jenekhe, *J. Mater. Chem*. **21** (41), 16461 (2011)
[21] A Babel, S A Jenekhe, *JACS* **125** (45), 13656 (2003)
[22] H T Nicolai, M Kuik, G A H Wetzelaer, B de Boer, C Campbell, C Risko, J L Brédas, P W M Blom, *Nature Materials*, DOI 10.1038/NMAT3384 (2012)
[23] A Al Naim, M Grell, *Appl. Phys. Lett.* **101**, 141603 (2012)
[24] L Hague, D Puzzovio, A Dragoneas, M Grell, *Sci. Adv. Mater.* **3**, 907 (2011)
[25] H Usta, A Facchetti, T J Marks, *Accounts of Chemical Research* **7**, 501 (2011)
[26] L Hague, D Puzzovio, A Dragoneas, M Grell, *Sensor Letters* **3**, 907 (2011)
[27] A J Bard and L R Faulkner, *Electrochemical Methods: Fundamentals and Applications* (2nd ed.), 2001 John Wiley & Sons Inc.
[28] A Al Naim, M Grell, *J. Appl. Phys.* **112***, 114502 (2012)*
[29] http://www.brukerafmprobes.com/Product.aspx?ProductID=3603